Supporting Information

Orientation of Fluorinated Cholesterol in Lipid Bilayers Analyzed by ^{19}F Tensor Calculation and Solid-State NMR

Nobuaki Matsumori,* Yusuke Kasai, Tohru Oishi, Michio Murata, Kaoru Nomura

Department of Chemistry, Osaka University, 1-1 Machikaneyama, Toyonaka, Osaka 560-0043, Japan.

Suntory Institute for Bioorganic Research, 1-1-1 Wakayamadai, Shimamoto-Cho, Mishima-Gun, Osaka 618-8503, Japan.

Table of Contents

Complete list of Reference 31	S2
Table S1. Cartesian coordinates of the optimized structure	S3
Table S2. Calculated ^{19}F shielding tensor elements (ppm)	S4
Table S3. Principal axes and principal shielding values of ^{19}F	S4
Figure S1. ^{13}C–^{19}F REDOR of 6-F-cholesterol in DMPC (dephasing 0.571 ms)	S5
Figure S2. ^{13}C–^{19}F REDOR of 6-F-cholesterol in DMPC (dephasing 1.142 ms)	S6
Figure S3. ^{2}H NMR spectra of 3-^{2}H-cholesterol in powder state and in DMPC	S7

Complete list of reference 31.

Frisch, M. J.; Trucks, G. W.; Schlegel, H. B.; Scuseria, G. E.; Robb, M. A.; Cheeseman, J. R.; Montgomery, J. A. Jr.; Vreven, T.; Kudin, K. N.; Burant, J. C.; Millam, J. M.; Iyengar, S. S.; Tomasi, J.; Barone, V.; Mennucci, B.; Cossi, M.; Scalmani, G.; Rega, N.; Petersson, G. A.; Nakatsuji, H.; Hada, M.; Ehara, M.; Toyota, K.; Fukuda, R.; Hasegawa, J.; Ishida, M.; Nakajima, T.; Honda, Y.; Kitao, O.; Nakai, H.; Klene, M.; Li, X.; Knox, J. E.; Hratchian, H. P.; Cross, J. B.; Adamo, C.; Jaramillo, J.; Gomperts, R.; Stratmann, R. E.; Yazyev, O.; Austin, A. J.; Cammi, R.; Pomelli, C.; Ochterski, J. W.; Ayala, P. Y.; Morokuma, K.; Voth, G. A.; Salvador, P.; Dannenberg, J. J.; Zakrzewski, V. G.; Dapprich, S.; Daniels, A. D.; Strain, M. C.; Farkas, O.; Malick, D. K.; Rabuck, A. D.; Raghavachari, K.; Foresman, J. B.; Ortiz, J. V.; Cui, Q.; Baboul, A. G.; Clifford, S.; Cioslowski, J.; Stefanov, B. B.; Liu, G.; Liashenko, A.; Piskorz, P.; Komaromi, I.; Martin, R. L.; Fox, D. J.; Keith, T.; Al-Laham, M. A.; Peng, C. Y.; Nanayakkara, A.; Challacombe, M.; Gill, P. M. W.; Johnson, B.; Chen, W.; Wong, M. W.; Gonzalez, C.; Pople, J. A. *Gaussian 03*, revision B.05; Gaussian, Inc.: Pittsburgh, PA, 2003.

Table S1. Cartesian coordinates of the optimized structure used for the tensor calculation

Center Number	Atomic Number	Atomic Type	Coordinates (Angstroms)		
			X	Y	Z
1	6	0	−1.277954	1.029417	−0.012823
2	6	0	−0.047988	0.566642	0.201932
3	9	0	−1.524947	2.376155	0.047999
4	6	0	−2.512986	0.250637	−0.327134
5	6	0	0.252127	−0.932116	0.093230
6	1	0	−3.337097	0.638224	0.282032
7	6	0	−2.294349	−1.245452	−0.074315
8	1	0	−2.800936	0.432955	−1.371422
9	1	0	−3.082958	−1.827505	−0.560489
10	1	0	−2.378299	−1.449451	0.997945
11	6	0	1.525439	−1.122073	−0.777527
12	6	0	−0.919310	−1.677267	−0.589673
13	6	0	0.492222	−1.524923	1.501939
14	1	0	0.769407	−2.581723	1.430551
15	1	0	−0.404075	−1.452583	2.122216
16	1	0	1.293493	−1.012573	2.037704
17	1	0	−0.783904	−2.756932	−0.462035
18	1	0	−0.877804	−1.486708	−1.668981
19	1	0	1.807328	−2.181808	−0.768307
20	6	0	2.714966	−0.248197	−0.362245
21	1	0	1.269334	−0.880517	−1.816512
22	1	0	3.548745	−0.417373	−1.052244
23	1	0	3.079696	−0.542163	0.629207
24	6	0	2.326898	1.233707	−0.352131
25	1	0	3.167193	1.850245	−0.015550
26	6	0	1.104038	1.483472	0.546502
27	1	0	2.092453	1.554939	−1.374617
28	1	0	1.397775	1.320218	1.592572
29	1	0	0.785536	2.524265	0.479422

Table S2. Calculated ^{19}F shielding tensor elements (ppm)

XX = 277.4355	YX = 20.5594	ZX = −26.9780
XY = 9.6182	YY = 353.0108	ZY = −4.4034
XZ = −26.7130	YZ = −7.3309	ZZ = 387.3610

The shielding tensor can be deconvoluted into a symmetric ($\boldsymbol{\sigma}^{s}$) and antisymmetric ($\boldsymbol{\sigma}^{as}$) component, and the symmetric component $\boldsymbol{\sigma}^{s}$ of the above tensor is given by:

$$\begin{pmatrix} 277.4355 & 15.0888 & -26.8455 \\ 15.0888 & 353.0108 & -5.86715 \\ -26.8455 & -5.86715 & 387.3610 \end{pmatrix}$$

The eigenvalues and eigenvectors of the symmetric part of the shielding tensor correspond to the principal values and principal axes, respectively.

Table S3. Principal axes and principal shielding values of ^{19}F

	Principal axes			Principal values (ppm)
	x	y	z	
σ_{11}	0.964517	−0.15864	0.211041	269.0798
σ_{22}	0.104394	0.963358	0.247069	353.1412
σ_{33}	-0.2425	−0.21627	0.945737	395.5864

σ_{ISO} = 339.2691 ppm, Anisotropy = 84.4760 ppm

Note that, in the text, we used chemical shift values (δ) instead of shielding values (σ).

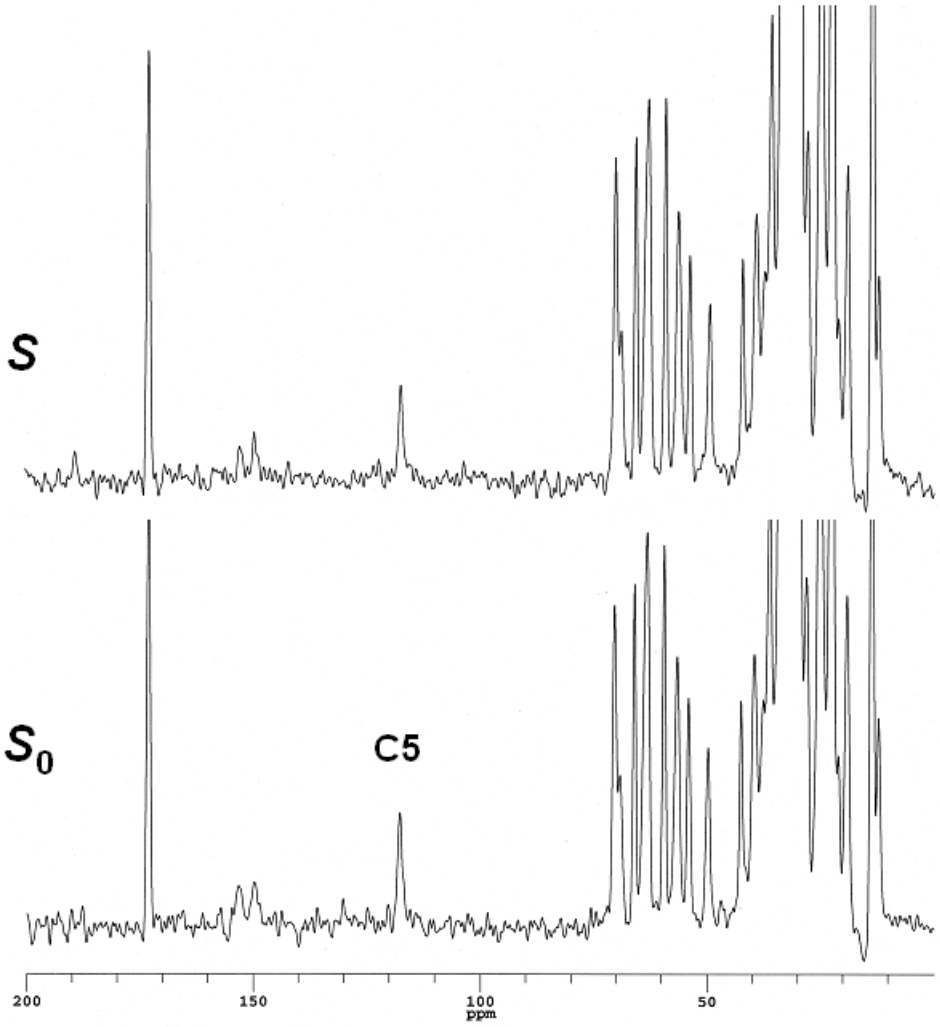

Figure S1. $^{13}C-^{19}F$ REDOR spectrum of 30 mol % 6-F-cholesterol in DMPC membrane. The spectra were obtained after 4 rotor cycles of ^{19}F dephasing (0.571 ms) with the magic angle spinning at 7 kHz at 30 °C. The number of the scans was 16000. The top and bottom traces are the full echo spectrum, S_0, and the dephased spectrum, S. The dephasing value $(S_0-S)/S_0$ at C5 is 0.22.

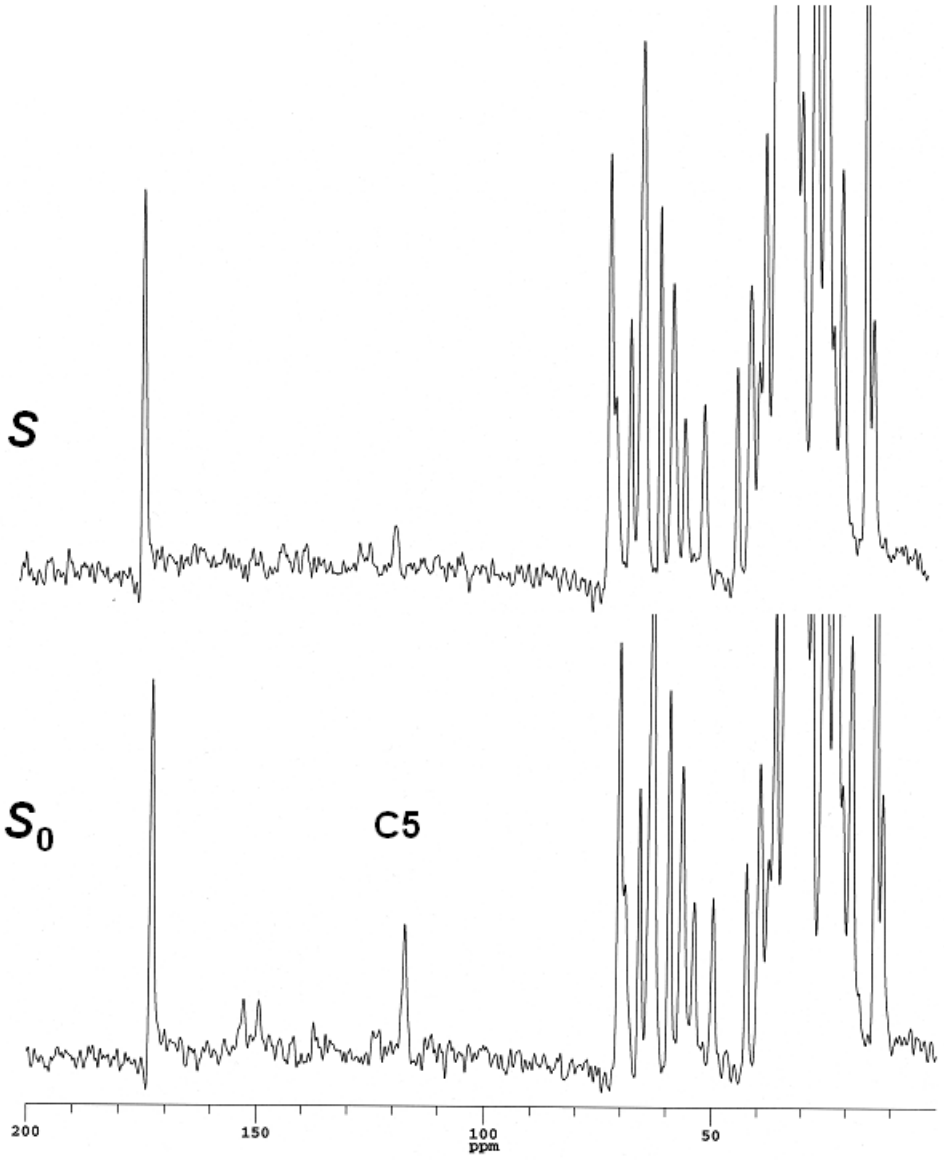

Figure S2. $^{13}C-^{19}F$ REDOR spectrum of 30 mol % 6-F-cholesterol in DMPC membrane. The spectra were obtained after 8 rotor cycles of ^{19}F dephasing (1.142 ms) with the magic angle spinning at 7 kHz at 30 °C. The number of the scans was 17600. The top and bottom traces are the full echo spectrum, S_0, and the dephased spectrum, S. The dephasing value $(S_0-S)/S_0$ at C5 is 0.71.

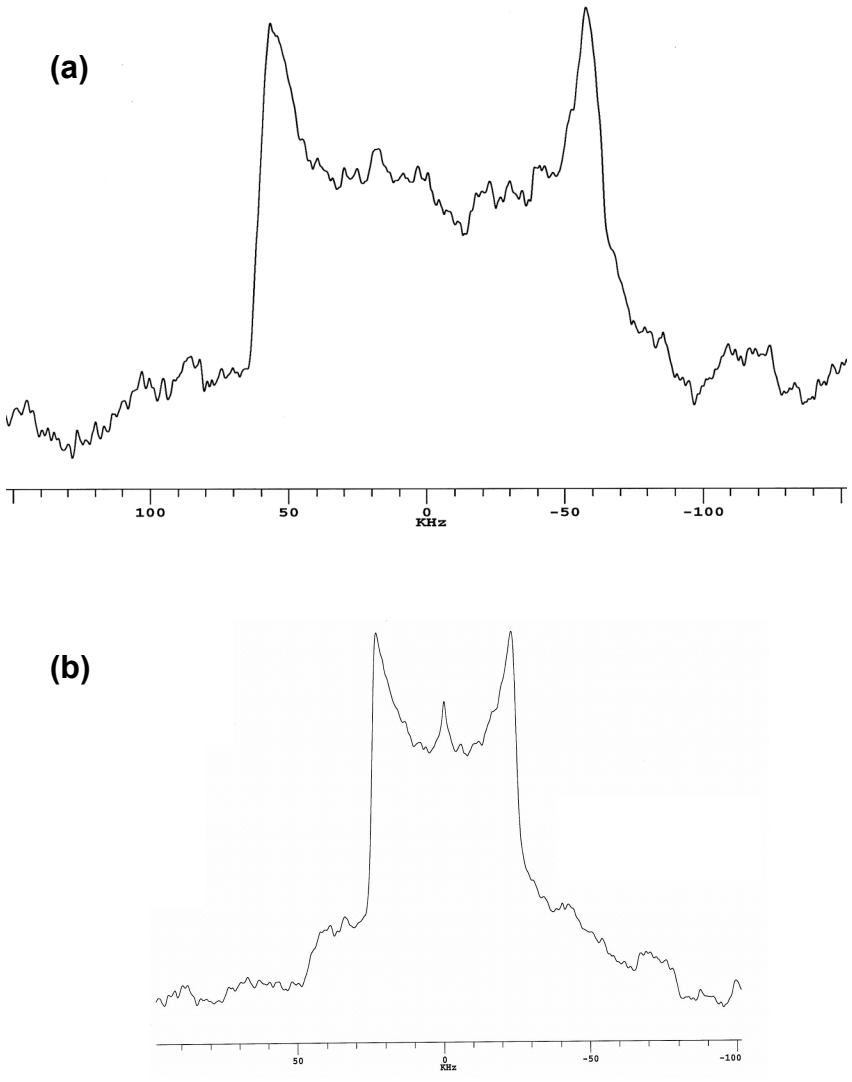

Figure S3. ^{2}H-NMR spectra of 3-^{2}H-cholesterol in powder state (a) and in DMPC bilayers (b). Spectra recorded at 30 ºC, using quadrupolar echo sequence. Quadrupolar splittings $\Delta\nu$ are 114 kHz (a) and 46 kHz (b). Most papers use more than 120 kHz for static C-^{2}H quadrupolar couplings, which was reported for aliphatic methylene deuterium of paraffin (*JCP*, **1971**, *55*, 5829). This difference may be explained by the dependence of the quadrupolar coupling constant on the polarization of the C-^{2}H bond induced by electronegative OH group.